

MICROCOPY RESOLUTION TEST CHART
 NATIONAL BUREAU OF STANDARDS
 (STANDARD REFERENCE MATERIAL 1010a)
 (ANSI and ISO TEST CHART No. 2)

ISTITUTO NAZIONALE DI FISICA NUCLEARE

Sezione di Catania

IT9200017

INFN/TC-91/05
24 Aprile 1991

F. Riggi:

**DESIGN OF A REFLEX TIME-OF-FLIGHT MASS SPECTROMETER
FOR THE STUDY OF THE DESORPTION OF MOLECULAR IONS**

**DESIGN OF A REFLEX TIME-OF-FLIGHT MASS SPECTROMETER
FOR THE STUDY OF THE DESORPTION OF MOLECULAR IONS**

F.Riggi

INFN - Sezione di Catania, Corso Italia 57, I95129 Catania, Italy
and

**Dipartimento di Fisica, Universita' di Catania, Corso Italia 57, I95129
Catania, Italy**

ABSTRACT

A reflex time-of-flight mass spectrometer for the study of the desorption and dissociation of molecular ions has been designed. A general overview of the instrument is reported, together with the different experimental aspects of the technique. These include mechanical and vacuum solutions, secondary ion optics in the electrostatic mirror, electronics, data acquisition and analysis.

1. - INTRODUCTION

Since the discovery in 1974 by MacFarlane and coworkers¹ that non volatile biomolecules can be ionized and desorbed by MeV/A heavy ions, this effect has been investigated both in fundamental studies on the desorption mechanism and for its application to different fields.

Many instrumental progresses have been made since that time and it is hoped that more detailed measurements of the desorbed products will contribute to the understanding of the process. One of such developments deals with the analysis of the correlation between the different secondary ions and/or neutrals resulting from each desorption event. Such correlated particles can originate from the desorption

process itself, since the number of secondary ions created in each event is generally larger than one. A large part of the correlated yield however results also from the metastable decay of the desorbed secondary ions which can undergo in-flight dissociation along the flight path.

Such studies have become possible in recent years²⁻⁴ with the use of electrostatic mirrors coupled to time-of-flight (TOF) mass spectrometers. The use of this reflectron allows measurements of daughter ion masses from parent ions which decompose during the first part of their flight path. A detector placed behind the mirror is able to measure the flight time of the resulting neutral fragments, while reflecting back ionized particles. This gives a better resolution on the identification of the parent ions. A correlated measure of these neutrals together with the charged fragments reflected at 180° , can be used to determine the possible fragmentation channels.

For this purpose a reflex time-of-flight instrument has been designed and it is presently under construction at our Institute. A general overview of the apparatus is given in the following, together with a discussion of several aspects involved in the design of the spectrometer. Among these, the mechanical part and vacuum system, the secondary ion optics along the flight path, the electronics and data acquisition are discussed.

2. - DESIGN OF THE INSTRUMENT

2.1 - General overview

A schematic lay-out of the instrument is shown in fig.1, which illustrates also the principle of the method.

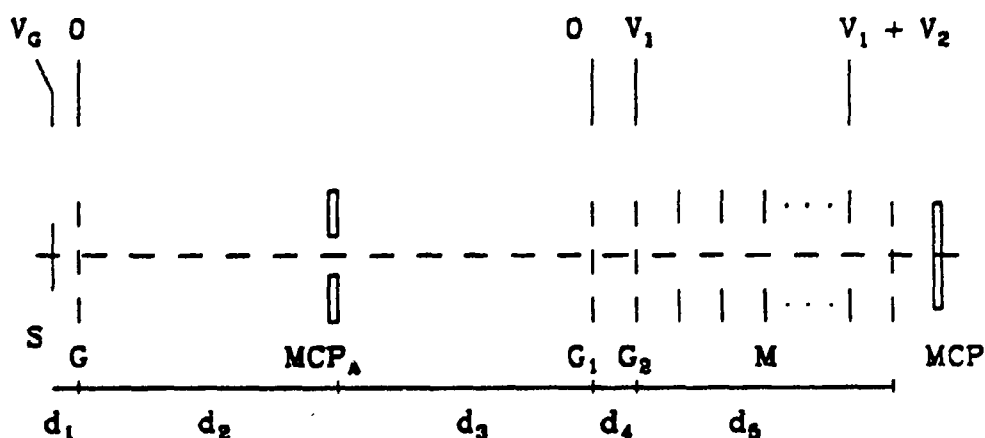


Fig. 1 - Schematic geometry of the reflex time-of-flight mass spectrometer.

A sample S, which is usually obtained by electrospraying a few μg of a solution onto a backing is placed at a few mm distance (d_1) from a high transparency grid G. The sample is at a high voltage $\pm V_G$ with respect to the grid, usually at ground potential. The ions emitted from the sample are then accelerated by this voltage difference and allowed to fly in a field-free region (length $d_2 + d_3$) down to a grid G_1 which is the entrance to an electrostatic mirror M. This includes a second grid G_2 (placed at d_4 from the first one) and a series of concentric parallel rings, placed at increasing voltages such as to maintain a uniform electric field in the central region. At the end of the flight path the microchannel-plate (MCP) detector stops the particles impinging on it, and gives a time signal for the time-of-flight measurement. A second microchannel-plate MCP_A (annular type) is placed along the flight path at a distance d_2 from the acceleration grid G. The secondary ion beam pass through the hole and the ions which are reflected from the electrostatic mirror can be then detected by the annular MCP, thus giving a second stop signal. The combination of these stop signals, together with a common start associated to the desorption event, will allow time correlation between the different ions and/or neutrals involved.

The geometry of the system and the electrostatic fields in the different sections of the spectrometer were studied through Monte Carlo simulation (see sect.3.3) in order to optimize both efficiency and mass resolution of the instrument.

2.2 - Mechanics and vacuum

The spectrometer will be installed inside a vacuum system which is made of a cylindrical vacuum chamber (DN320) coupled to a flight tube (length around 1 m) through one lateral flange. The pumping system installed at the rear end of the flight tube includes a 400 l. turbomolecular unit with a roughing pump. An additional primary pump is connected to the chamber for primary vacuum. The electrostatic mirror, placed at the end of the flight path, is installed in a second, smaller chamber and mechanically coupled to the flight tube. A cross placed along the flight path allows an easy access to the annular microchannel plate.

The sample holder is made parallel to the entrance grid of the flight tube. This is a critical point for mass resolution. The sample holder is mounted on a linear translational unit which is controlled by a step-by-step motor with 1μ resolution. The motor is coupled to a central unit, put outside the chamber and can be remotely controlled. The system allows then to place several samples in front of the accelerating grid without breaking the vacuum. Additional flanges on the chamber and along the flight tube allow vacuum control and voltages feedthrough.

2.3 - Secondary ion optics

In order to optimize the efficiency and the mass resolution of the spectrometer, a simulation of the response of the system was carried out by means of a Monte Carlo procedure. In the calculations reported here, some of the geometrical parameters were assigned realistic values. Among these, the sample radius was assumed to be 3 mm. An annular MCP of radius 12.5 mm, with a central hole 4 mm diameter was considered. The distance d_1 between the sample and the accelerating grid was kept fixed (to 5 mm) as well as the distance between the different elements of the mirror (10 mm). The overall length of the mirror was chosen to be 130 mm. This leaves as free parameters the distances d_2 , d_3 and the voltages V_G , V_{G1} , V_{G2} .

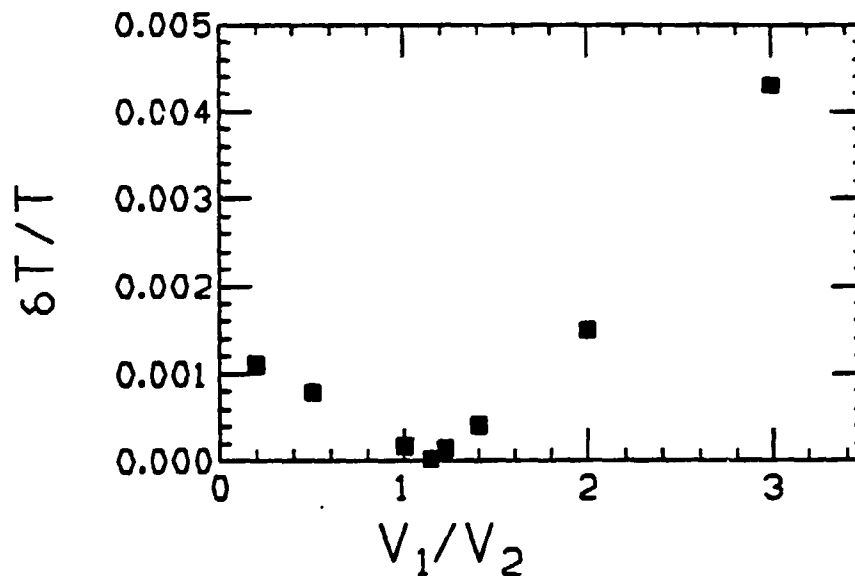


Fig. 2 - The relative time difference between ions emitted at rest and ions having an axial energy of 20 eV is reported as a function of V_1/V_2 .

Secondary ions having a maximum kinetic energy of 20 eV were assumed and the maximum difference between ions emitted at rest and ions emitted with an axial energy of 20 eV was first considered. The electric fields inside the mirror can contribute to improve the time resolution, with a proper choice of the voltages applied to the grid G_2 (the grid G_1 is grounded). As an example if we assume $d_2=d_3=400$ mm and $V_1+V_2=\text{fixed} \geq V_G$, the maximum time-of-flight difference between ions emitted at rest and ions having an axial energy of 20 eV varies with the ratio V_1/V_2 as in fig.2. The best situation is then obtained with $V_1/V_2 = 1.15$, i.e.

with a larger electric field in the first section of the mirror. In these conditions the mirror is able to compensate to some extent the effect of the different ion velocities. With a value of the ratio V_1/V_2 fixed to near its optimal value (1.15) the time resolution was seen to vary with the ratio d_2/d_3 as in fig.3. The best results are then expected when the annular MCP is placed in the middle of the field-free region.

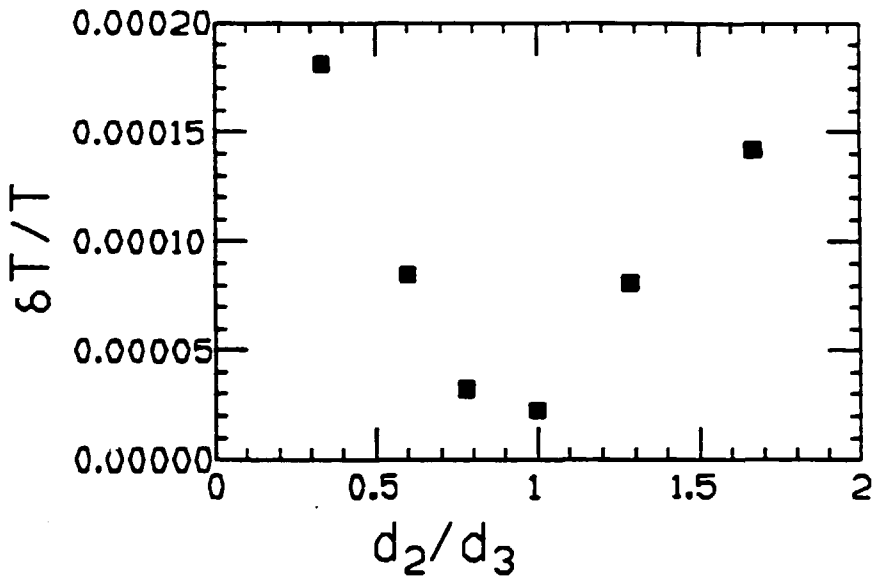


Fig. 3 - The same quantity as in fig.2 is reported as a function of d_2/d_3 , while the voltages V_1, V_2 are such that $V_1/V_2=1.15$.

When using long flight paths it is also important to optimize the detection efficiency in order not to lose too many secondary ions. This is particularly important in this case since a fraction of the desorbed ions is lost due to the size of the annular MCP and an additional fraction may be lost due to the reflection process. To simulate the response of the instrument a realistic shape was assumed to describe the initial energy distribution of the desorbed secondary ions.⁵ The overall detection efficiency (fraction of secondary ions being detected by the MCP_A after reflection in the mirror) is reported in fig.4 as a function of d_2/d_3 , for $d_2 + d_3 = 800$ mm and $V_1/V_2=1.15$.

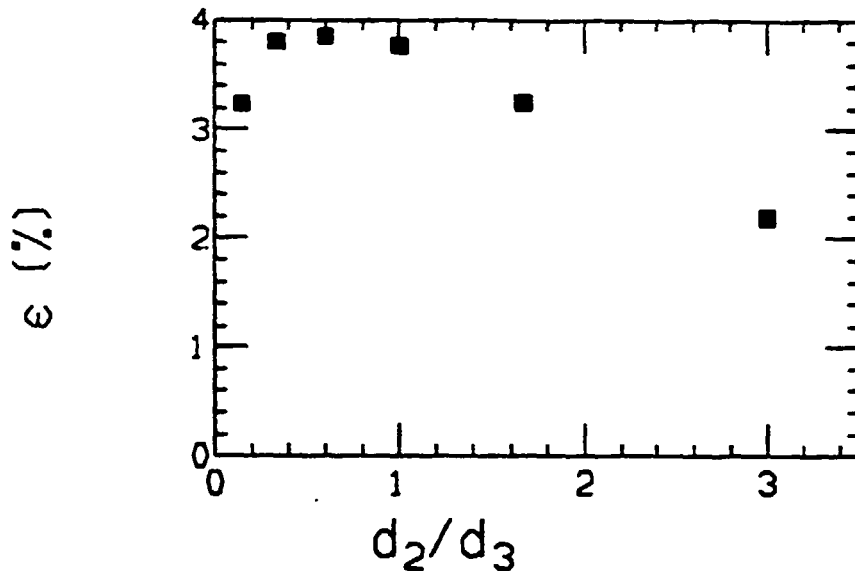


Fig. 4 - Geometrical detection efficiency as a function of d_2/d_3 , for $d_2 + d_3 = 800$ mm, and $V_1/V_2 = 1.15$. The other geometrical parameters are fixed as described in sect.2.3.

Fig.4 shows that in these conditions the efficiency is nearly constant for d_2/d_3 between 0.4 and 1 and it is slightly decreasing for d_2/d_3 outside this range. In these conditions the fraction of events passing through the hole of the annular MCP is only slightly higher (5.5% against 3.8%) than the overall efficiency, so that the reflection process does not contribute too much to losing events, and the detection efficiency is determined mainly by the geometry and ion optics in the first section of the spectrometer. Of course the absolute total length of the flight path influence both the efficiency and mass resolution which can be achieved. As an example fig.5 shows how the efficiency decreases with the (equal) lengths of the two sections.

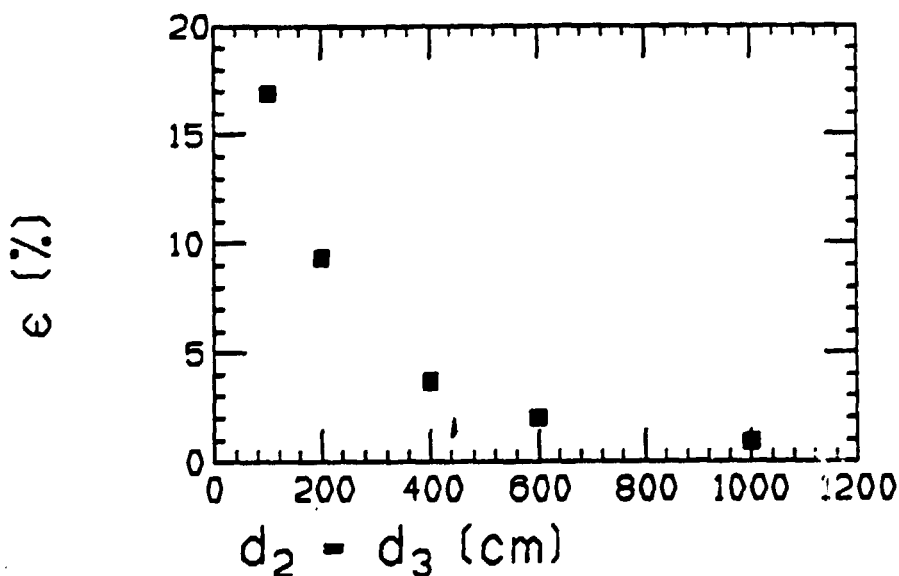


Fig. 5 - Geometrical detection efficiency as a function of the (equal) lengths of the two sections of the field-free region.

Whether a smaller flight path has to be chosen to improve the detection efficiency depends on the range of masses one is interested in, since the mass resolution is usually improving with the length of the flight path. In case of an electrostatic mirror however particular choices of the total length can compensate at least partially the effect of the initial energy distribution. As an example fig.6 shows simulated time-of-flight distributions in the reflex spectra of secondary ions, for different lengths of the two sections of the field-free region. The overall result from these simulations shows that a realistic choice of the geometry of the system is to assume equal lengths for the two sections and that an absolute value around 400 mm is a good compromise between efficiency and mass resolution. Of course other choices are possible, depending on the particular performance to be obtained.

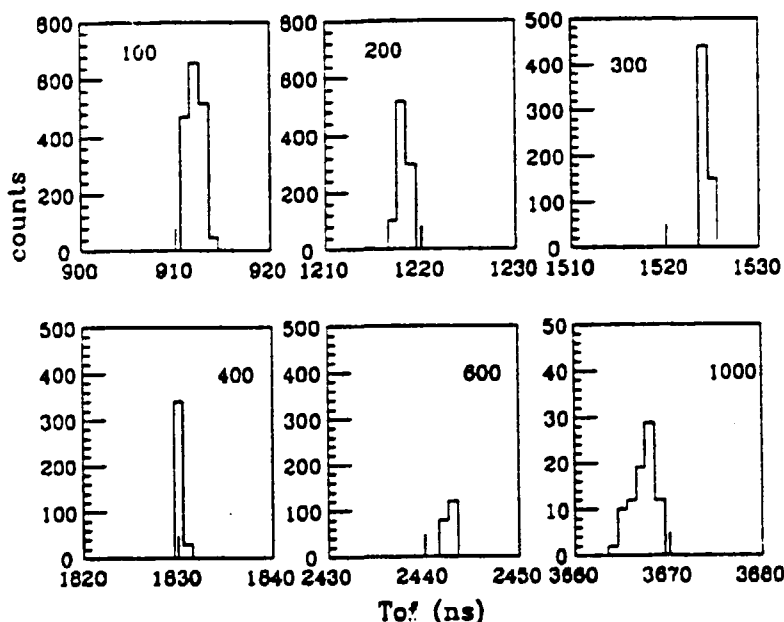


Fig. 6 - Time-of-flight simulated spectra of reflected secondary ions for different lengths of the two sections of the field-free regions.

2.4 - Electronics and data acquisition

A standard time-of-flight mass spectrometer usually requires only a monoparametric acquisition system. This is obtained by coupling a multistop time-to-digital converter to some acquisition device, like a multichannel analyzer or a computer through a suitable interface. In case of a reflex TOF spectrometer a multiparametric acquisition system is mandatory, even if the multidimensional capabilities

could be useful also in case of standard TOF technique, due to the secondary ion multiplicity larger than one.

The parameters to be collected and analyzed are in this case the arrival time on the MCP detector at the end of the flight path and the arrival time on the annular MCP detector. The first one, when the mirror is active, will give the neutral spectrum, while the second TOF will be used to build up the reflex charged spectrum. Event-by-event collection of these parameters will allow all the required correlations to be investigated. Since in each desorption event the number of emitted ions is usually larger than one, two multistop TDC's are required in order not to lose the knowledge of the event. Fig.7 gives a block diagram of the electronics and acquisition which will be used. FA and CFD are standard fast amplifier and constant fraction discriminators.

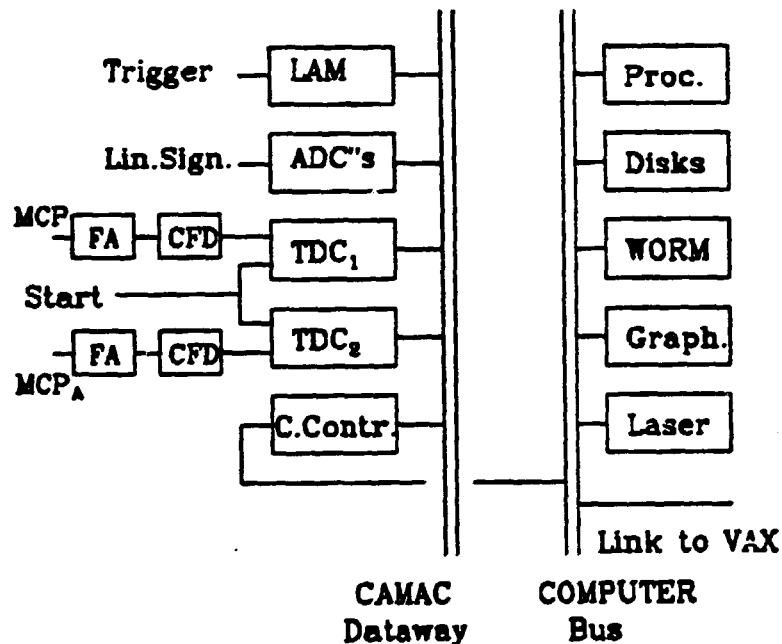


Fig. 7 - Block diagram of the electronics and data acquisition for the reflex time-of-flight mass spectrometer.

The TDC's are multistop devices (LeCroy 4208⁶ or units from IPN, Orsay⁷ to be read through CAMAC FIFO interface). Additional ADC's may be provided for linear signals. The LAM unit receives a trigger signal which can be generated by the start signal or by any logic coincidence of the signals involved. The CAMAC readout is based on the Crate Controller Kinetic System plus the interface⁸ to an IBM compatible computer. The processor is a 286-16 MHz with the mathematical coprocessor 80287, EGA color graphics card and a 40 Mb hard disk. An additional

WORM optical disk drive (200 Mb) will be used for mass storage of the events. A link to a VAX computer is also planned. The acquisition and analysis program was implemented in Fortran language with calls to CAMAC and graphics routines, by suitable modification of the software CAMDA⁹. This allows to store data event-by-event on disk and visualize and control on-line the status of monoparametric spectra. Two-dimensional live display is also possible. Apart from standard one-dimensional analysis (centroid, integral of peaks,...), one and two-dimensional windows can be chosen to select the events of interest. The acquisition rate is in the range of a few hundred events per second.

3. - STATUS OF THE PROJECT

All the main components of the spectrometer are ready except for the sample positioning system and the electrostatic mirror, under construction. All the vacuum components, including the pumping system, are already installed. The geometry and electrostatic properties of the system have been designed according to the considerations reported in sect.2.3 and the relevant parts (mirror, flight tube and sample positioning) are presently under construction or already commissioned. The electronics and data acquisition system is already installed and tested. It is planned to have then all the equipment installed and tested within the end of 1991.

REFERENCES

- (1) D.F.Torgerson, R.P.Skowronski and R.D.MacFarlane, *Biochem. Biophys. Res. Comm.* 60(1974)616.
- (2) S.Della Negra and Y.Le Beyec, *Anal.Chem.* 57(1985)2035.
- (3) X.Tang et al., *Anal.Chem.* 60(1988)1791.
- (4) K.G.Standing et al., *J.de Physique C2*(1989)163.
- (5) F.Riggi, *Nucl.Instr. and Methods B31*(1988)588.
- (6) LeCroy, 700 Chestnut Ridge Road, Chestnut Ridge, NY 10977-6499, USA.
- (7) E.Festa and R.Sellem, *Nucl.Instr. and Methods* 188(1981)99.
- (8) Kinetic System Corporation, 11 Maryknoll Drive, Lockport, Illinois 60441, USA.
- (9) H.Stelzer, A Camac-PC Data Acquisition System, Rossdorfer Str. 40, 6101 Messel, Germany.